MOX–Report No. 25/2007

Space-Time Adaption for Advection-Diffusion-Reaction Problems on Anisotropic Meshes

Stefano Micheletti, Simona Perotto

MOX, Dipartimento di Matematica "F. Brioschi"
Politecnico di Milano, Via Bonardi 29 - 20133 Milano (Italy)

mox@mate.polimi.it http://mox.polimi.it

Space–Time Adaption for Advection-Diffusion-Reaction Problems on Anisotropic Meshes

S. Micheletti, S. Perotto

5th December 2007

MOX– Modellistica e Calcolo Scientifico
Dipartimento di Matematica "F. Brioschi", Politecnico di Milano
via Bonardi 9, I-20133 Milano, Italy
{stefano.micheletti,simona.perotto}@polimi.it

Keywords: Space-time adaptivity; Anisotropic meshes; Time dependent problems:

AMS Subject Classification: 65M50, 65M15, 65M60

Abstract

We deal with the approximation of an unsteady advection-diffusion-reaction problem by means of space-time finite elements, continuous affine in space and piecewise constant in time. In particular, we are interested in the advection-dominated framework. To face the trade-off between computational cost and accuracy, we devise a space-time adaptive procedure where both the time step and the spatial grid are adapted throughout the simulation. Two are the key points involved: the derivation of an a posteriori error estimator where the contributions of the spatial and of the temporal discretization are split; a balance of these two contributions via a proper adaptive scheme. The main novelty of the paper is the interest for an anisotropic mesh adaption framework.

1 Introduction

Time dependent advection-dominated problems represent an interesting benchmark for an adaption procedure, due to the (possible) presence of steep internal and/or boundary layers, moving in time. We tackle this issue starting from a theoretically sound space-time adaptive procedure which: i) extends to the time dependent case the anisotropic interpolation error estimates in [7, 8]; ii) generalizes the a posteriori analysis in [13] for a pure diffusive problem to an advective-diffusive-reactive regime. Concerning the pertinent literature, an effective space-time adaptive procedure is proposed in [11] in an optimization framework. In this last case the authors focus on an isotropic goal-oriented analysis for the heat equation. Instead we pursue an anisotropic management of the space adaption procedure. Moreover we control a suitable energy norm of the discretization error as, e.g., in [1, 5]. As far as we know, the only paper dealing with a parabolic problem in an anisotropic framework is [16]. Here the heat equation is considered in an optimal control framework: the time discretization is carried out via the standard backward Euler scheme and no sound time adaption procedure is addressed, in favor of a heuristic approach.

Let us focus on the model parabolic problem for $u = u(\vec{x}, t)$

$$\begin{cases} L\,u = \partial_t u - \nabla \cdot (D\nabla u) + \vec{b} \cdot \nabla u + \sigma\, u = f & \text{in } \Omega \times J, \\ u = 0 & \text{on } \Gamma_{\mathrm{D}} \times J, \\ D\nabla u \cdot \vec{n} = g & \text{on } \Gamma_{\mathrm{N}} \times J, \\ u = u_0 & \text{on } \Omega \times \{0\}, \end{cases} \tag{1}$$

where $J = (0, T]$, with $T > 0$, is the considered time span, Ω is a bounded polygonal domain in $\mathbb{R}^2$ with boundary $\partial\Omega$, Γ_{D} and Γ_{N} are nonoverlapping subsets of $\partial\Omega$, each comprising a whole number of sides of $\partial\Omega$ and such that $\partial\Omega = \overline{\Gamma}_{\mathrm{D}} \cup \overline{\Gamma}_{\mathrm{N}}$, and $\mathbf{n}$ is the unit outward normal vector to $\partial\Omega$. Moreover we make the following assumptions on the data: the source $f \in L^2(0, T; L^2(\Omega))$; the Neumann datum $g \in L^2(0, T; H^{1/2}_{00}(\Gamma_{\mathrm{N}})')$; the diffusion tensor $D \in [L^\infty(\Omega)]^{2\times 2}$ and satisfies the standard ellipticity condition; the advective field $\vec{b} \in [L^\infty(\Omega)]^2$ with $\nabla \cdot \vec{b} \in L^\infty(\Omega)$ and $\vec{b} \cdot \vec{n} \geq 0$ a.e. on Γ_{N}; the reaction term $\sigma \in L^\infty(\Omega)$ with $\gamma = \sigma - \frac{1}{2}\nabla \cdot \vec{b} \geq 0$ a.e. in Ω, while the initial condition $u_0 \in L^2(\Omega)$. Notice that the notation adopted for the function spaces is standard (cf. e.g., [10]). The weak solution to (1) belongs to the space $U = L^2(0, T; H^1_{\Gamma_{\mathrm{D}}}(\Omega)) \cap H^1(0, T; H^1_{\Gamma_{\mathrm{D}}}(\Omega)')$. It is well known that the space U is continuously embedded in $C^0([0, T]; L^2(\Omega))$ ([4]).

1.1 Managing the space-time

The adopted discrete formulation can be seen as a spatial approximation of a discontinuous in time, dG(0), formulation [17]. Let us first manage the time discretization. We partition the interval J by the time levels $0 = t_0 < t_1 < \ldots <$

$t_{N-1} < t_N = T$, and set $J_n = (t_{n-1}, t_n]$, $k_n = t_n - t_{n-1}$. We define the space-time slab $S_n = \Omega \times J_n$, with $n = 1, \ldots, N$. Due to the possible time discontinuity characterizing the dG(0) approximation, for suitable smooth functions $v(\cdot, t)$, we also define the values $v_m^{\pm} = \lim_{\varepsilon \to 0^+} v(\cdot, t_m \pm \varepsilon)$ and the corresponding temporal jump $[v]_m = v_m^+ - v_m^-$, with $m = 1, \ldots, N-1$. Then we introduce the function space $\mathcal{S}_k = \{v : (0,T] \to H^1_{\Gamma_{\rm D}}(\Omega) : v(\cdot,t)\big|_{J_n} = \psi(\cdot), \psi \in H^1_{\Gamma_{\rm D}}(\Omega)\}$, whose elements coincide with polynomials of degree zero in t on each interval J_n, with coefficients in $H^1_{\Gamma_{\rm D}}(\Omega)$. The functions in $\mathcal{S}_k$ can be discontinuous at each time level, with continuity from the left. Moreover, since $0 \notin J_1$, the value $v(\cdot, 0)$ has to be specified separately, $\forall v \in \mathcal{S}_k$.

To discretize the space we resort to a family of conformal decompositions of $\overline{\Omega}$ into triangles, such that there is always a vertex of the triangulation at the interface between $\overline{\Gamma}_{\rm D}$ and $\overline{\Gamma}_{\rm N}$ (see, e.g., [3]). The temporal discontinuity allows for the employment of a family $\{\mathcal{T}_{h_n}\}_{h_n}$ of meshes, possibly different on each space-time slab S_n, for $n = 1, \ldots, N$. In particular we define $\mathcal{T}_{h_n} = \{K_n\}$, with K_n triangle of diameter h_{K_n} and $h_n = \max_{K_n} h_{K_n}$, the prism $S_{K_n} = K_n \times J_n$ and its lateral surface $L_{K_n} = \partial K_n \times J_n$. We are now in a position to define the so-called cG(1)-dG(0) space, $\mathcal{S}_{hk} = \{v_{hk} \in \mathcal{S}_k : v_{hk}(\cdot,t)\big|_{J_n} = \psi_h(\cdot), \psi_h \in X^1_{h_n} \cap H^1_{\Gamma_{\rm D}}(\Omega)\}$, $X^1_{h_n}$ being the space of the finite elements of degree one associated with the mesh $\mathcal{T}_{h_n}$ (see, e.g., [6]). The continuity of the functions $v_{hk} \in \mathcal{S}_{hk}$ is guaranteed with respect to the space, while the discontinuity in time characterizing the space $\mathcal{S}_k$ is maintained.

In view of the cG(1)-dG(0) formulation of (1), we introduce the bilinear and linear forms $B_{\rm DG-GLS}(\cdot,\cdot)$ and $F_{\rm DG-GLS}(\cdot)$, given by

$$
\begin{aligned}
B_{\rm DG-GLS}(v,w) &= \sum_{n=1}^{N} \int_{S_n} \left\{ \partial_t v\, w + D\nabla v \cdot \nabla w + (\vec{b} \cdot \nabla v + \sigma v)\, w \right\} d\vec{x}dt \\
&+ \int_\Omega v_0^+ w_0^+ \, d\vec{x} + \sum_{m=1}^{N-1} \int_\Omega [v]_m w_m^+ \, d\vec{x} + \sum_{n=1}^{N} \sum_{K_n \in \mathcal{T}_{h_n}} \int_{S_{K_n}} \tau_{K_n} Lv\, Lw \, d\vec{x}dt, \\
F_{\rm DG-GLS}(w) &= \sum_{n=1}^{N} \Big\{ \int_{S_n} f w \, d\vec{x}dt + \int_{J_n} \int_{\Gamma_{\rm N}} g w \, dsdt \\
&+ \sum_{K_n \in \mathcal{T}_{h_n}} \int_{S_{K_n}} \tau_{K_n} f\, Lw \, d\vec{x}dt \Big\} + \int_\Omega v_0 w_0^+ \, d\vec{x},
\end{aligned}
\tag{2}
$$

respectively, $v_0 = v_0^- \in L^2(\Omega)$ being known. These forms already incorporate a Galerkin Least-Squares (GLS) stabilization [9] to deal with possible numerical instabilities; the $\tau'_{K_n}s$ are suitable anisotropic piecewise constant stabilization coefficients ([15]).
Notice that $[u]_m = 0$, $m = 1, \ldots, N-1$, while $u_0^+ = u_0^- = u_0(\cdot)$, as $u \in U$.

The GLS cG(1)-dG(0) discrete formulation of problem (1) is: find $u_{hk} \in \mathcal{S}_{hk}$ such that

$$
B_{\rm DG-GLS}(u_{hk}, v_{hk}) = F_{\rm DG-GLS}(v_{hk}) \quad \forall v_{hk} \in \mathcal{S}_{hk}, \tag{3}
$$

where v_0 in (2) is replaced by $u_h^0 \in X_{h_1}^1 \cap H_{\Gamma_{\rm D}}^1(\Omega)$, i.e., by a proper finite element approximation of the initial data u_0.

It can be proved that the space-time error $e_{hk} = u - u_{hk}$ associated with the approximation u_{hk} satisfies a slabwise Galerkin orthogonality condition with respect to the discrete space $\mathcal{S}_{hk}$.

The bilinear form $B_{\rm DG-GLS}$ induces the norm

$$
\begin{aligned}
|||w|||_{\rm DG-GLS}^2 = B_{\rm DG-GLS}(w,w) = \sum_{n=1}^{N} \Big\{ & \|D^{1/2}\nabla w\|_{[L^2(S_n)]^2}^2 + \|\gamma^{1/2} w\|_{L^2(S_n)}^2 \\
& + \frac{1}{2}\|(\vec{b}\cdot\vec{n})^{1/2} w\|_{L^2(J_n\times\Gamma_{\rm N})}^2 + \sum_{K_n\in\mathcal{T}_{h_n}} \|\tau_{K_n}^{1/2} L w\|_{L^2(S_{K_n})}^2 \Big\} \\
& + \frac{1}{2}\sum_{m=1}^{N-1} \|w_m^+ - w_m^-\|_{L^2(\Omega)}^2 + \frac{1}{2}\|w_0^+\|_{L^2(\Omega)}^2 + \frac{1}{2}\|w_N^-\|_{L^2(\Omega)}^2
\end{aligned} \tag{4}
$$

on the space $U \cup \mathcal{S}_k$ (see, e.g. [9, 14] for further details). This is the energy norm on which we base the a posteriori analysis below.

2 The anisotropic framework

With a view to the a posteriori analysis, we recall the basic ideas of the anisotropic setting introduced in [7]. Moreover, we generalize some of the anisotropic interpolation error estimates in [7, 8] to the unsteady case.

Given any slab S_n, $\mathcal{T}_{h_n} = \{K_n\}$ being the associated mesh, we extract the anisotropic information from the invertible affine map $T_{K_n} : \widehat{K} \to K_n$ from the reference triangle $\widehat{K}$ to the general element $K_n \in \mathcal{T}_{h_n}$, such that $K_n = T_{K_n}(\widehat{K}) = M_{K_n}\widehat{K} + \vec{t}_{K_n}$, where $M_{K_n} \in \mathbb{R}^{2\times 2}$ and $\vec{t}_{K_n} \in \mathbb{R}^2$ denote the Jacobian and the offset associated with T_{K_n}, respectively. Then we introduce the polar decomposition $M_{K_n} = B_{K_n} Z_{K_n}$ of M_{K_n} into a symmetric positive definite matrix $B_{K_n} \in \mathbb{R}^{2\times 2}$ and an orthogonal matrix $Z_{K_n} \in \mathbb{R}^{2\times 2}$, and we further factorize the matrix B_{K_n} in terms of its eigenvectors $\vec{r}_{i,K_n}$ and eigenvalues λ_{i,K_n}, for $i = 1, 2$, as $B_{K_n} = R_{K_n}^{\rm T} \Lambda_{K_n} R_{K_n}$, with $\Lambda_{K_n} = {\rm diag}\,(\lambda_{1,K_n}, \lambda_{2,K_n})$ and $R_{K_n}^{\rm T} = [\vec{r}_{1,K_n}, \vec{r}_{2,K_n}]$. Notice that Z_{K_n} and $\vec{t}_{K_n}$ do not play any role in providing anisotropic information as associated with a rigid rotation and a shift, respectively. We choose $\widehat{K}$ as the equilateral triangle inscribed in the unit circle, with centroid placed at the origin. For this choice, it is possible to completely describe the shape and the orientation of each element K_n through the quantities $\vec{r}_{i,K_n}$ and λ_{i,K_n}. The unit circle circumscribed to $\widehat{K}$ is mapped into an ellipse circumscribing K_n: the eigenvectors $\vec{r}_{i,K_n}$ and the eigenvalues λ_{i,K_n} provide us with the directions and the length of the semi-axes of such an ellipse, respectively. In particular, we measure the deformation of each element K_n by the so-called stretching factor $s_{K_n} = \lambda_{1,K_n}/\lambda_{2,K_n}$, assuming, without loosing generality, $\lambda_{1,K_n} \geq \lambda_{2,K_n}$, so that $s_{K_n} \geq 1$, the equality holding if and only if K_n is equilateral.

We now state the anisotropic interpolation error estimates used in the a posteriori analysis. We focus on the Lagrange interpolant $\Pi^1_{h_n} : C^0(\overline{\Omega}) \to X^1_{h_n}$. The local interpolant $\Pi^1_{K_n} : \Pi^1_{K_n}\big(v\big|_{K_n}\big) = (\Pi^1_{h_n} v)\big|_{Kn}$, for any $v \in C^0(\overline{\Omega})$, satisfies the following

Lemma 2.1 *Let $v\big|_{S_{K_n}} \in L^2(J_n; H^2(K_n)) \cap U$; then it holds*

$$\begin{aligned} &\|v - \Pi^1_{K_n} v\|_{L^2(S_{K_n})} \le \mathcal{C}_1 \mathcal{L}_{K_n}(v), \quad |v - \Pi^1_{K_n} v|_{H^1(S_{K_n})} \le \mathcal{C}_2 \mathcal{L}_{K_n}(v), \\ &|v - \Pi^1_{K_n} v|_{H^2(S_{K_n})} \le \mathcal{C}_3 \mathcal{L}_{K_n}(v), \quad \|v - \Pi^1_{K_n} v\|_{L^2(L_{K_n})} \le \mathcal{C}_4 \mathcal{L}_{K_n}(v), \quad (5) \end{aligned}$$

where $\mathcal{C}_1 = C_1$, $\mathcal{C}_2 = C_2 \lambda^{-1}_{2,K_n}$, $\mathcal{C}_3 = C_3 \left(\frac{\lambda^2_{1,K_n} + \lambda^2_{2,K_n}}{\lambda^2_{1,K_n} \lambda^2_{2,K_n}} \right)^{1/2}$, $\mathcal{C}_4 = C_4 \left(\frac{\lambda^2_{1,K_n} + \lambda^2_{2,K_n}}{\lambda^3_{2,K_n}} \right)^{1/2}$, $\mathcal{L}_{K_n}(v) = \Big[\sum_{i,j=1}^2 \lambda^2_{i,K_n} \lambda^2_{j,K_n} L^{ij}_{K_n}(v) \Big]^{1/2}$, *the constants C_i, for $i = 1, \cdots, 4$ depending on $\widehat{K}$ only. Moreover, $L^{ij}_{K_n}(v) = \displaystyle\int_{S_{K_n}} (\vec{r}^{\,\mathrm{T}}_{i,K_n} H_{K_n}(v) \vec{r}_{j,K_n})^2 \, d\vec{x}dt$, with $i, j = 1, 2$, while $H_{K_n}(v)$ denotes the Hessian matrix associated with v.*

Estimates (5) generalize the standard (isotropic) results, recovered when $\lambda_{1,K_n} \simeq \lambda_{2,K_n} \simeq h_{K_n}$.

3 The a posteriori error estimate

We provide an a posteriori error estimator, $\eta_{\mathrm{DG-GLS}}$, for the DG-GLS norm (4) of the discretization error e_{hk}. It is essentially a residual-based estimator, weighted by suitable recovered derivatives of the error itself, in the spirit of a Zienkiewicz-Zhu recovery procedure [18, 12]. We define the local residuals, distinguishing between spatial and temporal. For any $K_n \in \mathcal{T}_{h_n}$, with $n = 1, \cdots, N$, let

$$\rho_{K_n} = \big[f - L u_{hk} \big] \Big|_{S_{K_n}} \text{ and } j_{K_n} = \begin{cases} 0 & \text{on } (\partial K_n \cap \Gamma_D) \times J_n, \\ 2(g - D\nabla u_{hk} \cdot \vec{n}) & \text{on } (\partial K_n \cap \Gamma_N) \times J_n, \\ -[D\nabla u_{hk} \cdot \vec{n}] & \text{on } (\partial K_n \cap \mathcal{E}^n_h) \times J_n, \end{cases}$$

be the interior and boundary residual associated with the cG(1)-dG(0) approximation u_{hk}, respectively, with $\mathcal{E}^n_h$ the skeleton of $\mathcal{T}_{h_n}$ and $[D\nabla u_{hk} \cdot \vec{n}] = D\nabla u_{hk} \cdot \vec{n}_{K_n} + D\nabla u_{hk} \cdot \vec{n}_{K'_n}$ the jump of the diffusive flux across the internal interfaces of K_n, for $(\overline{K'_n} \cap \overline{K_n}) \cap \mathcal{E}^n_h \neq \emptyset$. Then we introduce the temporal and the initial residuals, $\mathcal{J}_n = [-u_{hk}]_n$ and $e^-_0 = u_0 - u^0_h$, respectively. The residual $\mathcal{J}_n$ merges the information coming from the different meshes $\mathcal{T}_{h_n}$ and $\mathcal{T}_{h_{n+1}}$. This inevitably entails a careful computation of this term. As a consequence of the dG(0) approximation, it is useful to introduce the time averaged residuals, $\overline{\rho}_{K_n} = k_n^{-1} \int_{J_n} \rho_{K_n}(\cdot, t)\, dt$ and $\overline{j}_{K_n} = k_n^{-1} \int_{J_n} j_{K_n}(\cdot, t)\, dt$, which play an important role in the forthcoming analysis.

We can state the main result of our a posteriori analysis.

Proposition 3.1 *Let $u \in U$ be the weak solution to (1) and let $u_{hk} \in \mathcal{S}_{hk}$ be the corresponding GLS cG(1)-dG(0) approximation, solution to (3). Then there exists a constant $C = C(\widehat{K})$ such that*

$$|||e_{hk}|||^2_{\mathrm{DG-GLS}} \simeq \eta^2_{\mathrm{DG-GLS}} = C \sum_{n=1}^{N} \sum_{K_n \in \mathcal{T}_{h_n}} \Big(\underbrace{\alpha^{\mathrm{S}}_{K_n} R^{\mathrm{S}}_{K_n} \omega^{\mathrm{S}}_{K_n}}_{\eta^{\mathrm{S}}_{K_n}} + \underbrace{\sum_{i=1}^{4} \alpha^{\mathrm{T}i}_{K_n} R^{\mathrm{T}i}_{K_n} \omega^{\mathrm{T}i}_{K_n}}_{\eta^{\mathrm{T}}_{K_n}} \Big), \tag{6}$$

where $\alpha^{\mathrm{S}}_{K_n} = |\widehat{K}|\, \lambda^2_{1,K_n}\, \lambda^2_{2,K_n}$, $\alpha^{\mathrm{T}i}_{K_n} = k_n^2$, $i = 1, \cdots, 4$,

$$R^{\mathrm{S}}_{K_n} = |K_n|^{-1/2} \Big\{ \|\overline{\rho}_{K_n}\|_{L^2(S_{K_n})} + (\lambda^2_{1,K_n} + \lambda^2_{2,K_n})^{1/2}\, \lambda^{-3/2}_{2,K_n}\, \|\overline{j}_{K_n}\|_{L^2(L_{K_n})}$$
$$+ k_n^{-1/2} (\|\mathcal{J}_{n-1}\|_{L^2(K_n)} + \delta_{1n} \|e_0^-\|_{L^2(K_n)}) + \tau_{K_n} \Big(\lambda^{-1}_{2,K_n} \|\vec{b} - \nabla \cdot D\|_{[L^\infty(K_n)]^2}$$
$$+ \|\sigma\|_{L^\infty(K_n)} + (\lambda^2_{1,K_n} + \lambda^2_{2,K_n})^{1/2} (\lambda_{1,K_n} \lambda_{2,K_n})^{-1} \|D\|_{[L^\infty(K_n)]^{2\times 2}} \Big) \|\overline{\rho}_{K_n}\|_{L^2(S_{K_n})} \Big\},$$

$$\omega^{\mathrm{S}}_{K_n} = |K_n|^{-1/2} \Big[s^2_{K_n}\, L^{11}_{K_n}(e^*_{hk}) + 2\, L^{12}_{K_n}(e^*_{hk}) + s^{-2}_{K_n}\, L^{22}_{K_n}(e^*_{hk}) \Big]^{1/2},$$

$$R^{\mathrm{T1}}_{K_n} = k_n^{-1/2} \Big[\|\rho_{K_n} - \overline{\rho}_{K_n}\|_{L^2(S_{K_n})} + k_n^{-1/2} \Big(\|\mathcal{J}_{n-1}\|_{L^2(K_n)} + \delta_{1n} \|e_0^-\|_{L^2(K_n)} \Big) \Big]$$
$$+ \tau_{K_n} \Big(\|\sigma\|_{L^\infty(K_n)} \|\rho_{K_n} - \overline{\rho}_{K_n}\|_{L^2(S_{K_n})} + k_n^{-1} \|\rho_{K_n}\|_{L^2(S_{K_n})} \Big) \Big],$$

$$R^{\mathrm{T2}}_{K_n} = (4k_n)^{-1/2} \|j_{K_n} - \overline{j}_{K_n}\|_{L^2(L_{K_n})}, \quad R^{\mathrm{T3}}_{K_n} = R^{\mathrm{T4}}_{K_n}\, \|\vec{b}\|_{[L^\infty(K_n)]^2},$$
$$R^{\mathrm{T4}}_{K_n} = \tau_{K_n} k_n^{-1/2} \|\rho_{K_n} - \overline{\rho}_{K_n}\|_{L^2(S_{K_n})},$$
$$\omega^{\mathrm{T1}}_{K_n} = k_n^{-1/2} \|\partial_t e^*_{hk}\|_{L^2(S_{K_n})}, \quad \omega^{\mathrm{T2}}_{K_n} = k_n^{-1/2} \|\partial_t e^*_{hk}\|_{L^2(L_{K_n})},$$
$$\omega^{\mathrm{T3}}_{K_n} = k_n^{-1/2} \|\partial_t \nabla e^*_{hk}\|_{[L^2(S_{K_n})]^2}, \quad \omega^{\mathrm{T4}}_{K_n} = k_n^{-1/2} \|\partial_t \nabla \cdot (D \nabla e^*_{hk})\|_{L^2(S_{K_n})},$$

where δ_{1n} is the Kronecker symbol, and all the terms depending on e^*_{hk} designate suitable space-time recovery quantities that provide computable spatial and temporal derivatives of the discretization error e_{hk}.

Further details concerning the space and time recovery procedures can be found, for instance, in [18] and [11], respectively, as well as in [14], where the complete proof of (6) is furnished too. We just remark that the quantities $R^{\mathrm{S}}_{K_n}$, $R^{\mathrm{T}i}_{K_n}$, with $i = 1, \cdots, 4$, are scaled (with respect to the size $|K_n|$ of the element and k_n of the time interval, respectively), so that all the spatial and temporal dimensional information is collected into the coefficients $\alpha^{\mathrm{S}}_{K_n}$, $\alpha^{\mathrm{T}i}_{K_n}$, respectively. The weights $\omega^{\mathrm{S}}_{K_n}$ are associated with the anisotropic source, whereas the $\omega^{\mathrm{T}i}_{K_n}$'s drive the time adaption procedure. Finally, $\eta^{\mathrm{S}}_{K_n}$ ($\eta^{\mathrm{T}}_{K_n}$) in (6) represent the local estimators for a pure space-dependent (time-dependent) problem.

3.1 The adaptive algorithm

The adaptive algorithm is the same as that introduced in [13]. An equidistribution in space-time of the total error is enforced by splitting a given tolerance τ, equal for each slab, into a space (τ^{S}) and a time (τ^{T}) contribution. The time step and the spatial mesh are successively adapted until both the estimators of the space and time error are within their respective tolerances, i.e., until $\eta_n^{\mathrm{S}} = \sum_{K_n \in \mathcal{T}_{h_n}} \eta_{K_n}^{\mathrm{S}} \simeq \tau^{\mathrm{S}}$, and $\eta_n^{\mathrm{T}} = \sum_{K_n \in \mathcal{T}_{h_n}} \eta_{K_n}^{\mathrm{T}} \simeq \tau^{\mathrm{T}}$. After processing a slab, if the time tolerance is largely satisfied, a new (larger) time step is guessed for the next slab. This algorithm is similar to that in [2] though in our case both space and time adaptivity are carried out via an optimization strategy rather than through a compute-estimate-mark-refine procedure.

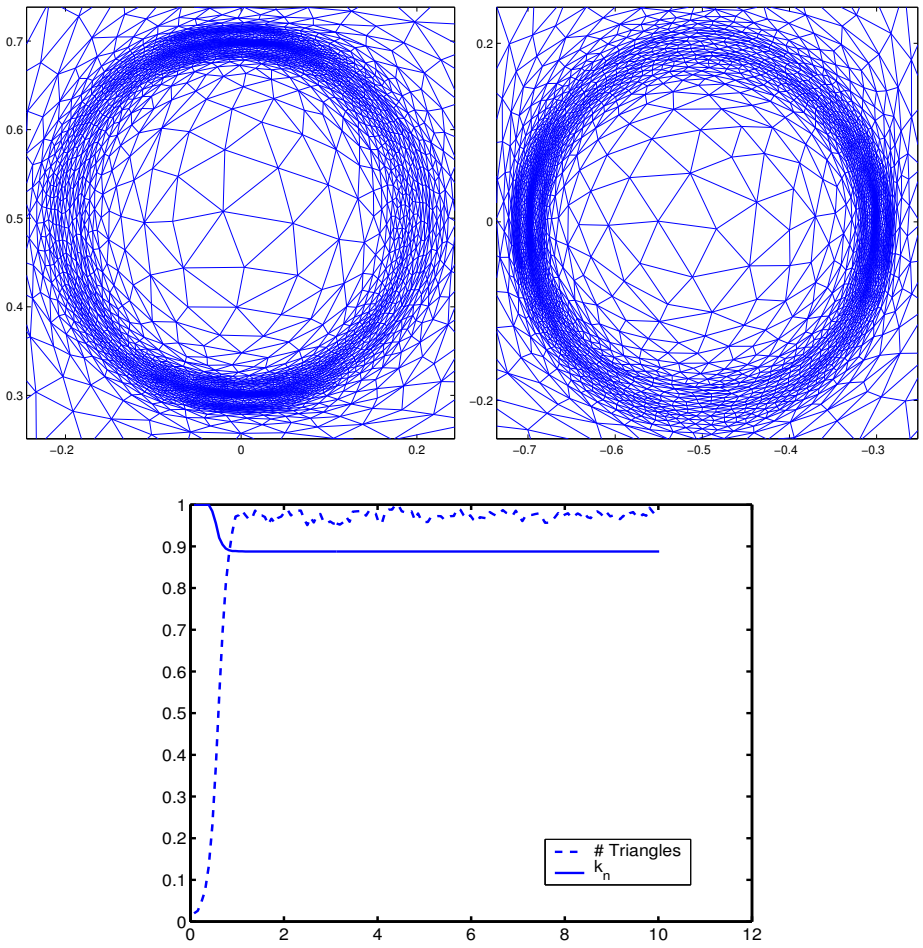

Figure 1: Details of the adapted meshes at $t \simeq T/4$ (top-left) and at $t \simeq T/2$ (top-right); time evolution of the time step k_n (solid) and of the number of mesh elements (dashed), scaled to their maximum value (bottom)

3.2 The rotating donut

We approximate problem (1) on the cylinder $\Omega \times J = (-1,1)^2 \times (0,10)$, with $D = 10^{-3} I$ (with I the identity tensor), $\vec{b} = [-x_2, x_1]^T$, $\sigma = 0$, $\Gamma_N = \emptyset$, and f, u_0 chosen such that $u = \exp\big(-((r - r_c)/\delta)^2\big)$, where $r = \sqrt{(x_1 - x_{1,R})^2 + (x_2 - x_{2,R})^2}$, $x_{1,R} = R\cos(\omega\, t), x_{2,R} = R\sin(\omega\, t)$, with $r_c = 0.2, \delta = 0.01, \omega = 2\pi/10, R = 0.5$. The exact solution is localized in an annular region of thickness $\mathcal{O}(\delta)$ rotating counterclockwise at a constant angular velocity ω. The tolerances for the adaptive algorithm are $\tau^S = \tau^T = 0.01$. Figure 1 shows a detail of the adapted meshes at $t \simeq T/4$ (top-left) and $t \simeq T/2$ (top-right). The mesh is correctly detecting the anisotropic features of the solution. In particular we can appreciate a sort of "wake" effect that is a clear effect of the donut velocity: this detail would not be spotted in the case of the corresponding stationary problem. The bottom graph in Figure 1 displays the time evolution of the time step k_n (solid) and of the number of mesh elements (dashed), scaled to their maximum value. These time histories show that, after a transient phase, both the time step and the number of triangles level out, as a consequence of the constant angular velocity and of the absence of distortion of the donut. At the final time we obtain the value 1.257 for the effectivity index $EI = \eta_{\mathrm{DG-GLS}}/|||e_{hk}|||_{\mathrm{DG-GLS}}$.

Concerning the future developments, we are currently extending the above analysis to an optimal control framework.

References

[1] Akrivis, G., Makridakis, C., Nochetto, R.: A posteriori error estimates for the Crank-Nicolson method for parabolic equations. Math. Comp. **75**, 511–531 (2006)

[2] Cascón, J.M., Ferragut, L., Asensio, M.I.: Space-time adaptive algorithm for the mixed parabolic problem. Numer. Math. **103**, 367–392 (2006)

[3] Ciarlet, P.: The Finite Element Method for Elliptic Problems. North-Holland, Amsterdam (1978)

[4] Dautray, R., Lions, J.L.: Mathematical Analysis and Numerical Methods for Science and Technology: Evolution Problems I, vol. 5. Springer-Verlag, Berlin (1992)

[5] Eriksson, K., Johnson, C.: Adaptive finite element methods for parabolic problems. I: a linear model problem. SIAM J. Numer. Anal. **28**, 43–77 (1991)

[6] Eriksson, K., Johnson, C., Thomée, V.: Time discretization of parabolic problems by the discontinuous Galerkin method. RAIRO Modelisation Math. Anal. Numer. **19**, 611–643 (1985)

[7] Formaggia, L., Perotto, S.: New anisotropic a priori error estimates. Numer. Math. **89**, 641–667 (2001)

[8] Formaggia, L., Perotto, S.: Anisotropic error estimates for elliptic problems. Numer. Math. **94**, 67–92 (2003)

[9] Hughes, T.J.R., Franca, L.P., Hulbert, G.M.: A new finite element formulation for computational fluid dynamics: VIII. The Galerkin/least-squares method for advective-diffusive equations. Comput. Methods Appl. Mech. Engrg. **73**, 173–189 (1989)

[10] Lions, J.L., Magenes, E.: Non-homogeneous boundary value problems and applications. Vol. I. Springer-Verlag, New York (1972)

[11] Meidner, D., Vexler, B.: Adaptive space-time finite element methods for parabolic optimization problems. SIAM J. Control Optim. **46**, 116–142 (2007)

[12] Micheletti, S., Perotto, S.: Reliability and efficiency of an anisotropic Zienkiewicz-Zhu error estimator. Comput. Methods Appl. Mech. Engrg. **195**, 799–835 (2006)

[13] Micheletti, S., Perotto, S.: Anisotropic mesh adaption for time-dependent problems. To appear in Internat. J. Numer. Methods Fluids (2008)

[14] Micheletti, S., Perotto, S.: In preparation (2008)

[15] Micheletti, S., Perotto, S., Picasso, M.: Stabilized finite elements on anisotropic meshes: a priori error estimates for the advection-diffusion and the Stokes problems. SIAM J. Numer. Anal. **41**, 1131–1162 (2003)

[16] Picasso, M.: Anisotropic a posteriori error estimate for an optimal control problem governed by the heat equation. Numer. Methods Partial Differential Equations **22**, 1314–1336 (2006)

[17] Thomée, V.: Galerkin finite element methods for parabolic problems. In: Springer Series in Computational Mathematics, vol. 25. Springer-Verlag, Berlin (2006)

[18] Zienkiewicz, O.C., Zhu, J.Z.: The superconvergent patch recovery and a posteriori error estimates. Part I: the recovery technique. Int. J. Numer. Methods Engrg. **33**, 1331–1364 (1992)

MOX Technical Reports, last issues

Dipartimento di Matematica "F. Brioschi",
Politecnico di Milano, Via Bonardi 9 - 20133 Milano (Italy)

25/2007 S. Micheletti, S. Perotto:
Space-Time Adaption for Advection-Diffusion-Reaction Problems on Anisotropic Meshes

24/2007 L.M. Sangalli, P. Secchi, S. Vantini, A. Veneziani:
A Case Study in Functional Data Analisys: Geometrical Features of the Internal Carotid Artery

23/2007 L.M. Sangalli, P. Secchi, S. Vantini, A. Veneziani:
Efficient estimation of 3-dimensional centerlines of inner carotid arteries and their curvature functions by free knot regression splines

22/2007 G.O. Roberts, L.M. Sangalli:
Latent diffusion models for event history analysis

21/2007 P. Massimi, A. Quarteroni, F. Saleri, G. Scrofani:
Modeling of Salt Tectonics

20/2007 E. Burman, A. Quarteroni, B. Stamm:
Stabilization Strategies for High Order Methods for Transport Dominated Problems

19/2007 E. Burman, A. Quarteroni, B. Stamm:
Interior Penalty Continuous and Discontinuous Finite Element Approximations of Hyperbolic Equations

18/2007 S. Micheletti, S. Perotto:
Output functional control for nonlinear equations driven by anisotropic mesh adaption. The Navier-Stokes equations

17/2007 A. Decoene, L. Bonaventura, E. Miglio, F. Saleri:
Asymptotic Derivation of the Section-Averaged Shallow Water Equations for River Hydraulics

16/2007 A. Quarteroni:
Modellistica Matematica e Calcolo Scientifico